euspen's 22nd International Conference & Exhibition, Geneva, CH, May/June 2022
www.euspen.eu

First prototype of a positioning device with subatomic resolution

Roman Hebenstreit[1], Karin Wedrich[2], Steffen Strehle[2], Eberhard Manske[3], René Theska[1]

[1]*Technische Universität Ilmenau, Department of Mechanical Engineering, Institute for Design and Precision Engineering, Precision Engineering Group*
[2]*Technische Universität Ilmenau, Department of Mechanical Engineering, Institute of Micro- and Nanotechnologies, Microsystems Technology Group*
[3]*Technische Universität Ilmenau, Department of Mechanical Engineering, Institute of Process Measurement and Sensor Technology*

roman.hebenstreit@tu-ilmenau.de

Abstract

In the forthgoing work on a device that enables subatomic resolved highly reproducible positioning, a first prototype is here presented. The entire positioning system including the actuator, sensor and guiding mechanism, is realized as a micro-electro-mechanical system (MEMS) on chip level, based on silicon-on-insulator (SOI) technology.
A modular printed circuit board acts as the mechanical as well as the electrical contacting interface for the silicon chip. First variants of a linear positioning system comprising axisymmetric double parallel crank structure are investigated. Pivot joints as flexure hinges with concentrated compliance are deployed. These hinges show minimal rotational axis displacement for small angles of deflection, thus ensuring smallest deviations to a straight-line path of the linear guiding mechanism. An electrostatic comb actuator transmits forces contactless to minimize over constraints. A measuring bridge in differential mode utilizes the same comb structures to measure the table position based on the capacitance change. Estimating the position resolution, limited by the resolution of the capacitive sensor, a measurable step width below 50 pm can be expected. In further steps, the device will be a platform to be equipped with a lattice-scale-based position measurement system according to achieve an even higher resolution and reproducibility.

Subatomic positioning, compliant mechanism, MEMS

1. Introduction

The following work intends to introduce the prototype of a positioning system which was presented in a concept paper in [1]. Combining the strengths of microsystems technology and Precision Engineering, the demonstrator enables unprecedented accuracy in a positioning system. For this purpose, the device is manufactured as a micro-electro-mechanical system (MEMS) in chip format based on silicon-on-insulator technology (SOI). The distinctive aspect here is the compactness of the device, whose footprint is no larger than a pinkie fingernail. This allows shortest loops to be achieved in the metrologically relevant structure. The material used, monocrystalline silicon, offers the benefit of having almost ideal elastic characteristics. Compared to conventional materials such as aluminium or steel alloys, it exhibits far less residual stresses. This enables predictable mechanical behaviour of the device over long periods of operation. Compliant mechanisms are used to ensure the highest possible guidance performance for this purpose.
The goal of this work is to provide a working linear positioning system as a feasible platform for the ongoing development of a lattice-scale-based position measurement system. In the following sections, the synthesized functional structure of the device is presented first. Subsequently, the focus is put on the methodology and description of the developed approaches to the partial functions of the positioning system based on electrostatic actuation and position detection. First results are presented on the integration of a scale entity, for the lattice-scale-based position measurement approach. Finally, an overview of the results and an outlook on further development goals is given.

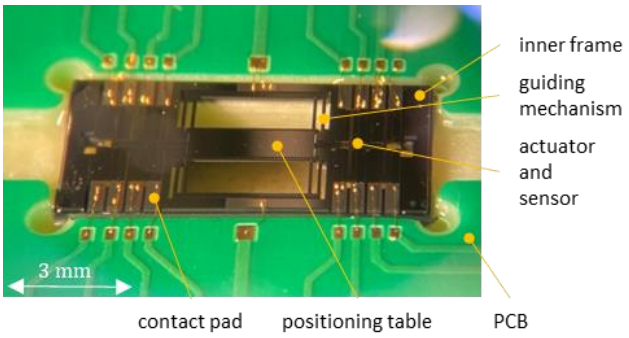

Figure 1 Image of PCB-mounted electrostatic positioning device

2. Functional structure

The development of a positioning device with subatomic resolution faces complex requirements. To enable a systematic approach the overall function of the positioning system is divided into sub-functions as shown in (Fig. 2). Two subsystems are initially distinguished here. First, there is the periphery used for signal processing as well as for a control interface between the system and the operator. This peripheric system is widely decoupled from the positioning system. The latter comprises, on the one hand, a lattice-scale-based position measurement system including an extended metrological frame, a mounting and a drive for the approach motion of the scanning probe microscope (SPM), which is intended for the pickup of active

cantilevers. On the other hand, there is the electrostatic positioning system. This includes the electrostatic actuator and position sensor, the compliant guiding mechanism and the positioning table. The table provides the interface for the scale entity. In the state presented here, the MEMS is mounted on a printed circuit board (PCB).

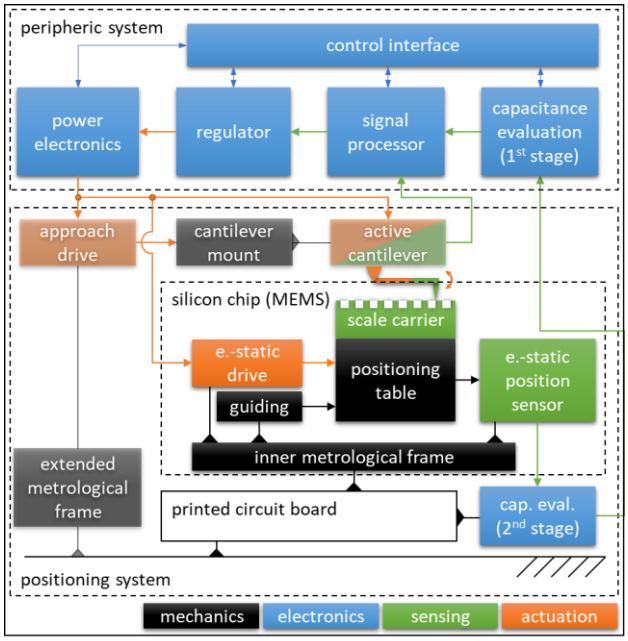

Figure 2 Scheme of functional structures

3. Electrostatic positioning system design

The entire structure of the MEMS is manufactured as a monolithic system. The underlying manufacturing process is derived from the flow chart as published in [2], which has been optimized for active MEMS based on SOI technology. In this technology, two silicon wafers (device and handle wafer) are bonded isolated by a thin silicon dioxide layer (buried oxide layer) to form an SOI wafer unit.

The functionally important structure of the positioning device is fabricated from monocrystalline silicon on the device layer, whereas the handle layer serves as the frame. The developed fabrication process is based on gas chopping and reactive deep ion etching. Structures with an aspect ratio of up to 1:20 can be reliably created [2]. Assuming a $100\ \mu m$ thick device layer, structures as thin as $5\ \mu m$ like the joints, for example, can be realized. An example from the first batch, a flexure hinge with $10\ \mu m$ thickness is shown in (Fig. 3).

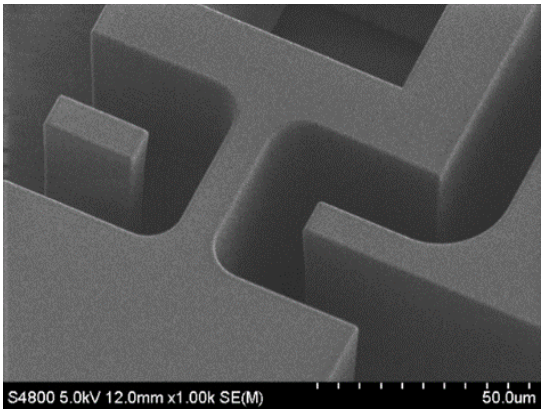

Figure 3. SEM image of flexure hinge with 10 µm thinnest section

The actuators and sensors described in the following sections must be electrically contacted individually. To insulate the conductive parts (channels) from each other, these structures must be separated on the device layer. Each channel is provided with at least one contact pad, which connects to the adjacency electronics. These are located on a PCB, which also serves as a socket for the MEMS chip (see Fig. 1). Gold wire bonding is used to create an electrical connection between them. Low ohmic contact pads of a metal stack with an aluminium and p-doped silicon interface [3] are deployed to minimize the effect of intrinsic thermal run-up during operation.

3.1. Guiding mechanism and table

The linear guiding mechanism satisfies the requirements from [1] by combining two self-compensating double-parallel crank mechanisms. The guided table is placed in the centre of the mechanism. The size is specified to $(3000 \times 1000)\ \mu m^2$. The chosen area size provides a sufficient platform for the transfer of scale substrates. Within the stroke of $\pm 10\ \mu m$, the guide shows a linear stiffness characteristic. The stroke is limited in both directions by hard end stops.

The method of pseudo-rigid body modelling (see Fig. 4) is used to lay out the total stiffness. The flexure hinges are modelled as compliant joints with a bending stiffness independent of the angle of rotation which is valid for small angles of deflection [4,5]. The individual stiffness of all 16 joints is assumed to be equal. The design of the individual joint stiffness is determined using the detasFlex programme [6] developed at the TU Ilmenau based on analytical model equations. This represents the fundament for the iterative design of the necessary drive force (see section 2.2) for the desired position resolution and the maximum addressable stroke before failure of the joints.

The results of the analytical stiffness calculation are compared with a non-linear 3D FEM reference model (ANSYS Workbench) of the guiding mechanisms with thoroughly modelled hinges for precision applications [7]. The results of the analytical and numerical stiffness calculations deviate from each other by less than $3\ \%$, which is within the acceptable range [8]. An important still unknown aspect of the described mechanisms is the deviation of the real joint widths from the modelled nominal values due to the manufacturing process. Also, for the contour of the joints, this deviation has a strong influence on the expected value of the stiffness. Therefore, four different designs are prepared to characterise this influence empirically. Shape deviations are estimated to have an evenly distributed effect on the overall geometry. Thus, the influence on the quality of the guide is assumed to be negligible.

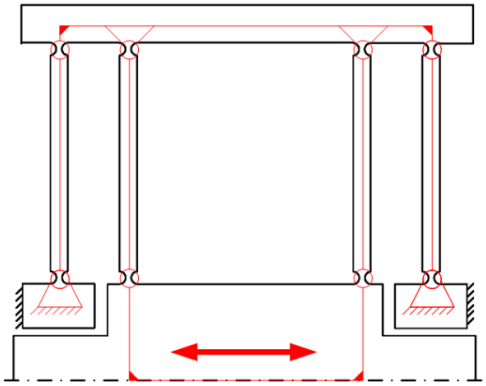

Figure 4. Schematic illustration of a half section of a pseudo-rigid body model of the guiding mechanism

3.2. Electrostatic drive

The electrostatic actuator comprises a comb structure with two stationary electrodes and the moving neutral electrode, which is fixed to the positioning table. This enables contactless induction of actuation forces as it is required for the precise motion of the positioning table [1]. In interaction with the overall stiffness of the guiding mechanism, a force-controlled actuation principle is obtained. The calculation of the necessary actuation force is iteratively coupled to the calculation of the stiffness of the guiding mechanism.
The goal is to achieve a stroke of $\pm\ 10\ \mu\mathrm{m}$ at a maximum voltage of $200\ \mathrm{V}$, as well as the highest resolution possible. A resolution of at least $100\ \mathrm{pm}$ has to be achieved. For the electrostatic principle of operation in the lateral mode of the comb actuator, the following relationship applies between the generated Coulomb force F_{actuator} and the voltage U [8].

$$F_{\mathrm{actuator}} = \frac{U^2 \cdot h \cdot \varepsilon_0 \varepsilon_{\mathrm{r}} \cdot n_{\mathrm{act}}}{2d} \qquad \{3.2.1\}$$

$$s = \frac{F_{\mathrm{actuator}}}{c_{\mathrm{guiding}}} = \frac{U^2 \cdot h \cdot \varepsilon_0 \varepsilon_{\mathrm{r}} \cdot n_{\mathrm{act}}}{2d \cdot c_{\mathrm{guiding}}} \qquad \{3.2.2\}$$

Where s is the position, represented by the sign and magnitude of the position vector of the table with respect to its neutral centre position, c_{guiding} is the total stiffness of the compliant guiding, h is the plate height, d is the spacing of the electrodes, n_{act} is the number of effective electrode gaps and ε_{r} and ε_0 describe the permittivity.
The secondary goal of the iterative dimensioning between the drive and the compliant guide mechanism is to achieve a minimum footprint of the MEMS chip. The spacing and height of the electrodes are set by manufacturing specifications. For this reason, the number of electrode teeth is considered a variable for optimisation. This scales proportionally with the area of the footprint.
The actuation voltage is generated in the first experimental setup using a *Keithley 2450 SourceMeter®* precision source, which allows steps of $\Delta U = 5\ \mathrm{mV}$ and an adjustment in the range of up to $U_{\mathrm{max}} = 200\ \mathrm{V}$. This corresponds to a relative resolution of 2.5×10^{-5} [9]. Inserted in Eq. 3.2.2 and derived with respect to the voltage, a linear characteristic of the resolution of the force-controlled actuator system is obtained with the slope $k = \Delta U \frac{h \cdot \varepsilon_0 \varepsilon_{\mathrm{r}} \cdot n_{\mathrm{act}}}{d \cdot c_{\mathrm{guiding}}}$. The step with the highest resolution is found around the zero point of the characteristic graph. This decreases linearly towards the outer limits of the control range. In differential operation of two oppositely coupled actuators, this behaviour can be improved, but not completely avoided. The position resolution of the actuator-guide combinations ranges from $6\ \mathrm{fm}$ to $550\ \mathrm{pm}$ within the addressable stroke of $\pm\ 10\ \mu\mathrm{m}$.

In the present configuration incorporating the compliant mechanism, restoring forces act on the system as a parasitic influence on the positioning performance. Thus, the approach of a position is not directly depending on the stiffness of the guiding mechanism. Additional energy buffers could balance out the stiffness depending on the position of the table [10]. Furthermore, a path-controlled drive principle should be targeted in further development. This could be realized by deploying an electrostatic stepper motor as it is shown exemplarily in [11] as a MEMS application**.**

3.3. Position Sensing

The electrostatic position sensor, like the actuator, is integrated directly into the MEMS. In this way, the metrological loop for the electrostatic positioning system is formed within the MEMS chip via the integral frame. Two stationary electrodes are placed on opposite sides to detect the direction of movement contactless. Between them, the neutral electrode can be found, which is rigidly attached to the positioning table and thereby also connected to the ground potential of the MEMS.

Each gap of the combs acts as a plate capacitor. The motion of the electrode causes a change in the capacitance. This is measured by an electronic evaluation system, which is divided into two stages. The first stage generates an alternating generator signal. This is divided into two measuring channels for the dynamic measurement of the capacitance between a stationary and the neutral electrode. In the second stage of the evaluation electronics, the differential signal of the two channels is generated. This is then transmitted back to the first stage, where it is amplified and read out by the control interface. Only the electronic components of the second stage are placed directly on the circuit board in which the MEMS is mounted (see Fig. 5). Heat sources near the stage can be minimised by placing the first stage thermally decoupled in the peripheric system.

Such an evaluation electronics ideally allows a resolution of the differential capacitance of up to $5\ \mathrm{aF}$. The geometry and a number of up to 600 combs per channel result in a position resolution of the electrostatic system of approx. $50\ \mathrm{pm}$. The ratio between the capacitive base load and the variable capacitance is approx. 10^{-6}. The total capacitance of the circuit between the second stage and the moving capacitor should be limited to approx. $5\ \mathrm{pF}$. Significant influences on this arise from the overlapping of the capacitor plates in the neutral middle position and parasitic capacitances on lines and contacts of the PCB and the MEMS itself. Furthermore, various noise sources must be considered and appropriate methods have to be elaborated to avoid and compensate parasitic capacitances and noise sources on the sensor signal.

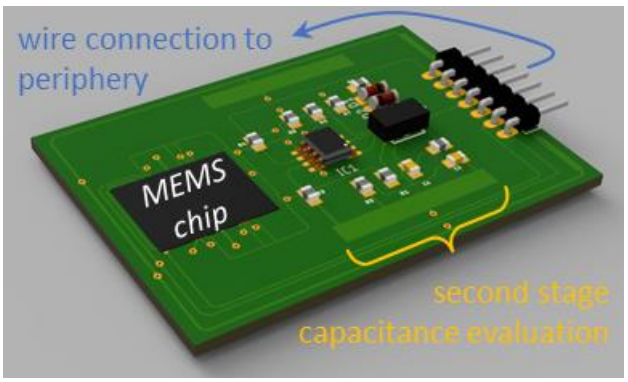

Figure 5. 3D model of PCB for mounting of MEMS, capacitance evaluation electronics, and connection to the peripheric system

4. Results and further steps

The upcoming work aims for the integration of the lattice-scale-based measurement system into the positioning system, as outlined in [1]. In the long term, even higher resolutions should be achievable that can be metrologically traced back to the lattice constant of crystalline scale entities.

Based on the functional structure in (Fig. 2), it is necessary to have a carrier for the scale entity. In the simplest case, this can be the substrate of the MEMS in which periodic structures are created. As a first approach, line patterns with a pitch of 200 nm and a depth of approx. 0.25 µm were etched directly in the positioning table using focused ion beam (FIB) etching. First results are shown in (Fig. 6). Due to the storage of silicon under ambient conditions, a thin native silicon-oxide layer is formed that in principle must be also considered.

The variety of other available manufacturing processes for the direct fabrication of nanostructures is rather limited, because the exposed microstructures of the MEMS are mechanically highly sensitive. A promising approach seems to be the transfer of a separate chip as a carrier for the scale entity. Hence, this chip could individually serve as a platform for a wider choice of processes for nanomaterials as scale entities. The challenge here, however, is the development of a suitable joining technique between the carrier chip and the positioning table. Studies on the transfer of compatible materials to microstructures are already in progress.

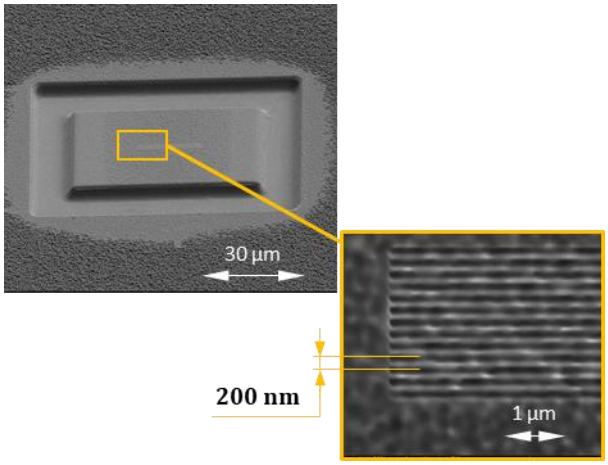

Figure 6. SEM image of FIB-structured periodic lines as a scale on the surface area of the positioning table

5. Summary

A first prototype of a linear positioning device with subatomic resolution is presented here for a stroke of ± 10 µm and an absolute positioning resolution extending into the femtometer range. A force-controlled drive principle is used, which is based on electrostatic force generation. The position is measured by evaluating the variable capacitance of a moving plate capacitor. Both sensor and actuator are comb-shaped structures made from an SOI wafer by using conventional microtechnologies. The kinematic loop of the electrostatic positioning system is closed within the inner frame of the MEMS device.
In further work, the device error will be determined empirically and influences on the accuracy will be systematised and characterised. The main focus will be on the calibration of the actuator and sensor behaviour as well as the signal conditioning of the measurement systems. The developed system represents the basis for the subsequent extension to a lattice-scale-based position measurement system. This requires the integration of an extended frame, which enlarges the metrological loop compared to the electrostatic positioning system. An additional drive for the approach of the measuring tip to the scale is required.
As a first preliminary work for the integration of a scale, line patterns have been generated in the silicon substrate of the positioning table by using FIB. Due to the lack of long-term stability of the material, more suitable materials and manufacturing processes for scale entities must be applied in the future. If necessary, the substrate of the scale carrier may have to be processed separately and afterwards be attached to the positioning table.

Acknowledgements

The authors gratefully acknowledge the support by the Deutsche Forschungsgemeinschaft (DFG) in the framework of Research Training Group "Tip- and laser-based 3D-Nanofabrication in extended macroscopic working areas" (GRK 2182) at the Technische Universität Ilmenau, Germany.

References

[1] Hebenstreit R et al. 2020 Conceptional design of a positioning device with subatomic resolution and reproducibility *Proceedings of the euspen 20th International Conference & Exhibition (Virtual Conference)*
[2] Wedrich K et al. 2021 Conceptual Design of a Microscale Balance Based on Force Compensation. In: Zentner L, Strehle S (eds) *Microactuators, Microsensors and Micromechanisms. MAMM 2020. Mechanisms and Machine Science* **96** Springer, Cham. https://doi.org/10.1007/978-3-030-61652-6_9
[3] Hillingermann U 2004 Silizium-Halbleitertechnologie *Teubner* **4** 124-127 https://doi.org/10.1007/978-3-322-94072-8
[4] Howell L Magleby S Olsen B 2013 Handbook of compliant mechanisms *Wiley* 57-65 https://doi.org/10.1002/9781118516485.ch2
[5] Zentner L 2014 Nachgiebige Mechanismen *De Gruyter Oldenburg* 28-39 https://doi.org/10.1524/9783486858907
[6] Henning S Linß S Zentner L 2018 detasFLEX – A computational design tool for the analysis of various notch flexure hinges based on non-linear modeling *Mechanical Sciences* **9** 389-404 https://doi.org/10.5194/ms-9-389-201
[7] Torres M et al. 2018 On modeling the bending stiffness of thin semi-circular flexure hinges for precision applications *Actuators* **7** (art.86) https://doi.org/10.3390/act7040086
[8] Schomburg W K 2015 Introduction to Microsystem Design *Springer Verlag RWTHedition* **2** 161-172
[9] Tektronix Inc. (ed.) https://download.tek.com/datasheet/2450-Datasheet_1KW-60904-0.pdf (datasheet, 15 June 2022)
[10] Gallego J Herder J 2011 Criteria for the Static Balancing of Compliant Mechanisms *34th Annual Mechanisms and Robotics Conference* **2** 465-473 https://doi.org/10.1115/DETC2010-28469
[11] Sarjlic E et al. 2009 Single mask 3-phase electrostatic rotary stepper micromotor *TRANSDUCERS 2009 - 2009 International Solid-State Sensors, Actuators and Microsystems Conference* 1505-1508 https://doi.org/10.1109/SENSOR.2009.5285801